# Rer1 and calnexin regulate endoplasmic reticulum retention of a peripheral myelin protein 22 mutant that causes type 1A Charcot-Marie-Tooth disease

Taichi Hara, Yukiko Hashimoto, Tomoko Akuzawa, Rika Hirai, Hisae Kobayashi, and Ken Sato*

Laboratory of Molecular Traffic, Institute for Molecular and Cellular Regulation, Gunma University, Maebashi, Gunma 371-8512, Japan

*Corresponding author:
Ken Sato
3-39-15 Showa-machi, Maebashi, Gunma 371-8512, Japan.
Tel: +81-27-220-8840
Fax: +81-27-220-8844
E-mail: sato-ken@gunma-u.ac.jp

Supplementary Information:

Supplementary Figure Legends

Figure S1

Figure S2

Figure S3

Figure S4

Figure S5

Figure S6

Original blots

**Supplementary Figure Legends**

**Figure S1. Subcellular localization of peripheral myelin protein 22 (PMP22)-GFP in HeLa cells stably expressing wild-type or mutant PMP22-GFP.**

A portion of wild-type (WT) PMP22-GFP (GFP, green fluorescent protein) colocalizes with late endosome/lysosome marker protein in HeLa cells. HeLa cells stably expressing WT or mutant PMP22-GFP were immunostained with an anti-Rab7 antibody and observed using confocal laser scanning microscopy. Scale bar, 10 μm.

**Figure S2. Knockdown of *Hrd1* using small interfering RNA (siRNA #1) increases the protein level of mutant PMP22-GFP.**

HeLa cells stably expressing WT or mutant PMP22-GFP were treated with control or *Hrd1* siRNA (Hrd1 #1) for 3 days. Immunoblots of cell lysates were probed with anti-GFP, anti-Hrd1, anti-gp78, and anti-α-actin antibodies. Note that Hrd1 #1 also reduced the protein level of gp78, suggesting that this siRNA has an off-target effect on *gp78* to some extent.

**Figure S3. Effect of *Hrd1*, *gp78*, and *calnexin* knockdown on PMP22 degradation.**

(A, C, E) Pulse-chase experiments of PMP22-GFP in HeLa cells. HeLa cells stably expressing PMP22(WT)-GFP (A), PMP22(L16P)-GFP (C), or PMP22(G150D)-GFP (E) were treated with control siRNA or siRNAs against *Hrd1*, *gp78*, or *calnexin (CNX)* for 3 days. To inhibit protein synthesis, we incubated cells in the presence of 10 μg/mL cycloheximide (CHX) for the indicated time. The cell lysates were immunoblotted with anti-GFP (top panel) and anti-α-actin (bottom panel) antibodies. (B, D, F) Quantitative analysis of the levels of each PMP22-GFP during pulse-chase experiments. Graphs show the relative level of PMP22(WT)-GFP (B), PMP22(L16P)-GFP (D), and PMP22(G150D)-GFP (F) normalized against α-actin. Values indicate the mean ±

standard error of the mean of three independent experiments. Two-way analysis of variance (ANOVA) was used to determine the significance of the differences. *$P < 0.05$ (ANOVA), **$P < 0.01$ (ANOVA).

**Figure S4. Effect of *Rer1* knockdown on the ER retention of PMP22(L16P) in COS1 cells.**

(A) Localization of PMP22-GFP derivatives in COS1 cells. COS1 cells stably expressing WT or mutant PMP22-GFP were transfected with control or *Rer1* siRNA for 3 days. Then, cells were fixed and observed using confocal laser scanning microscopy. Scale bar, 20 μm. (B) Immunodetection of PMP22-GFP in COS1 cells. COS1 cells stably expressing WT or mutant PMP22-GFP were treated with control or *Rer1* siRNA for 3 days. Immunoblots of total cell lysates were probed with anti-GFP (top panel), anti-Rer1 (middle panel), and anti-α-actin antibodies (bottom panel).

**Figure S5. Validation of the phenotype specificity induced by *Rer1* knockdown.**

Overexpression of mouse *Rer1* using a construct that lacked the sequence complementary to the cognate siRNA (Rer1 #7) rescued the phenotype induced by *Rer1* knockdown. HeLa cells stably expressing PMP22(L16P)-GFP were transfected with monomeric red fluorescent protein (mRFP)-mouse Rer1 (mRer1) using a retrovirus vector. Cells were treated with control siRNA or siRNA (Rer1 #7) against *Rer1*. Fixed cells were observed using confocal laser scanning microscopy. Scale bars, 10 μm.

**Figure S6. Localization of PMP22(G150D)-GFP to the ER was superficially unaffected by simultaneous knockdown of *Rer1* and *calnexin*.**

HeLa cells stably expressing PMP22(G150D)-GFP were treated with control or siRNA against *Rer1*, *calnexin*, or both for 3 days. Then, fixed cells were immunostained using an antibody against Lamp1 (a late endosome/lysosome marker) and observed using

confocal laser scanning microscopy. Scale bars, 10 μm.

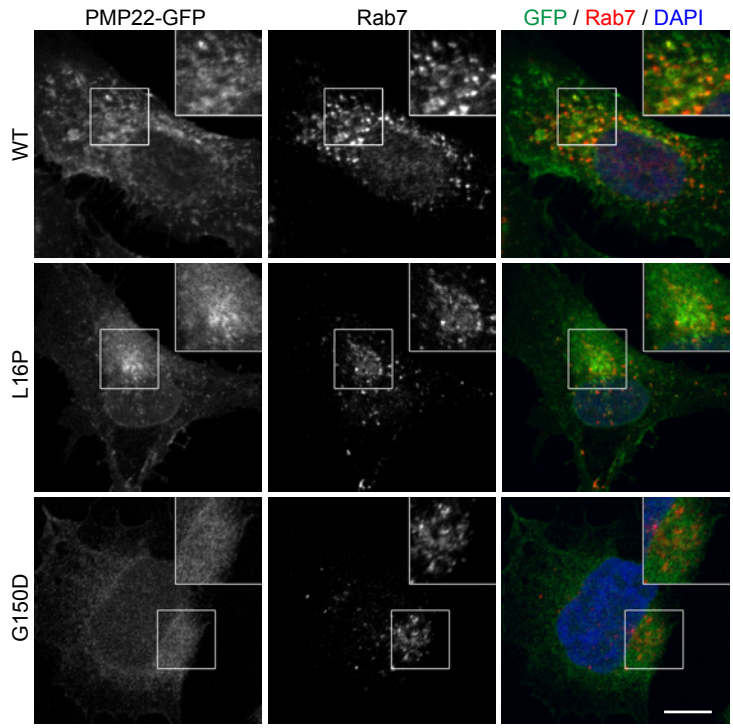


**Figure S1. Subcellular localization of peripheral myelin protein 22 (PMP22)-GFP in HeLa cells stably expressing wild-type or mutant PMP22-GFP.**

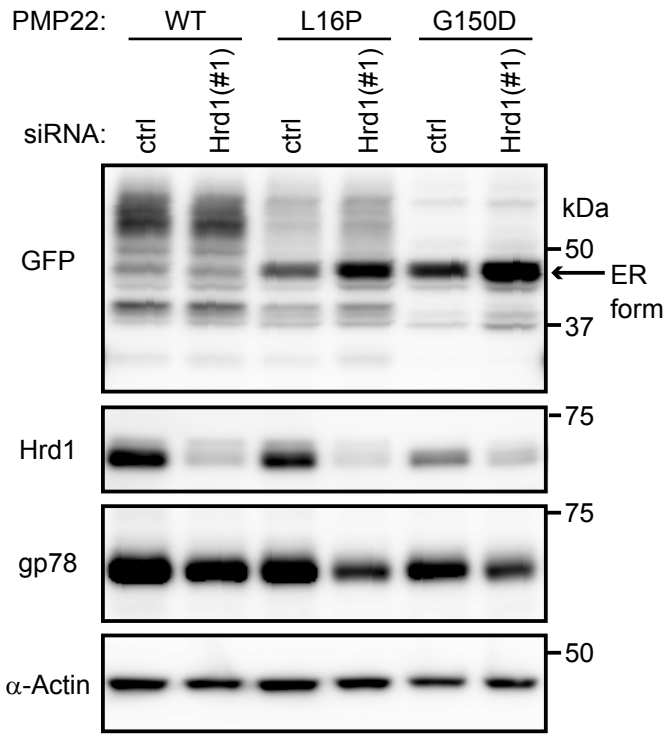


**Figure S2. Knockdown of *Hrd1* using small interfering RNA (siRNA #1) increases the protein level of mutant PMP22-GFP.**

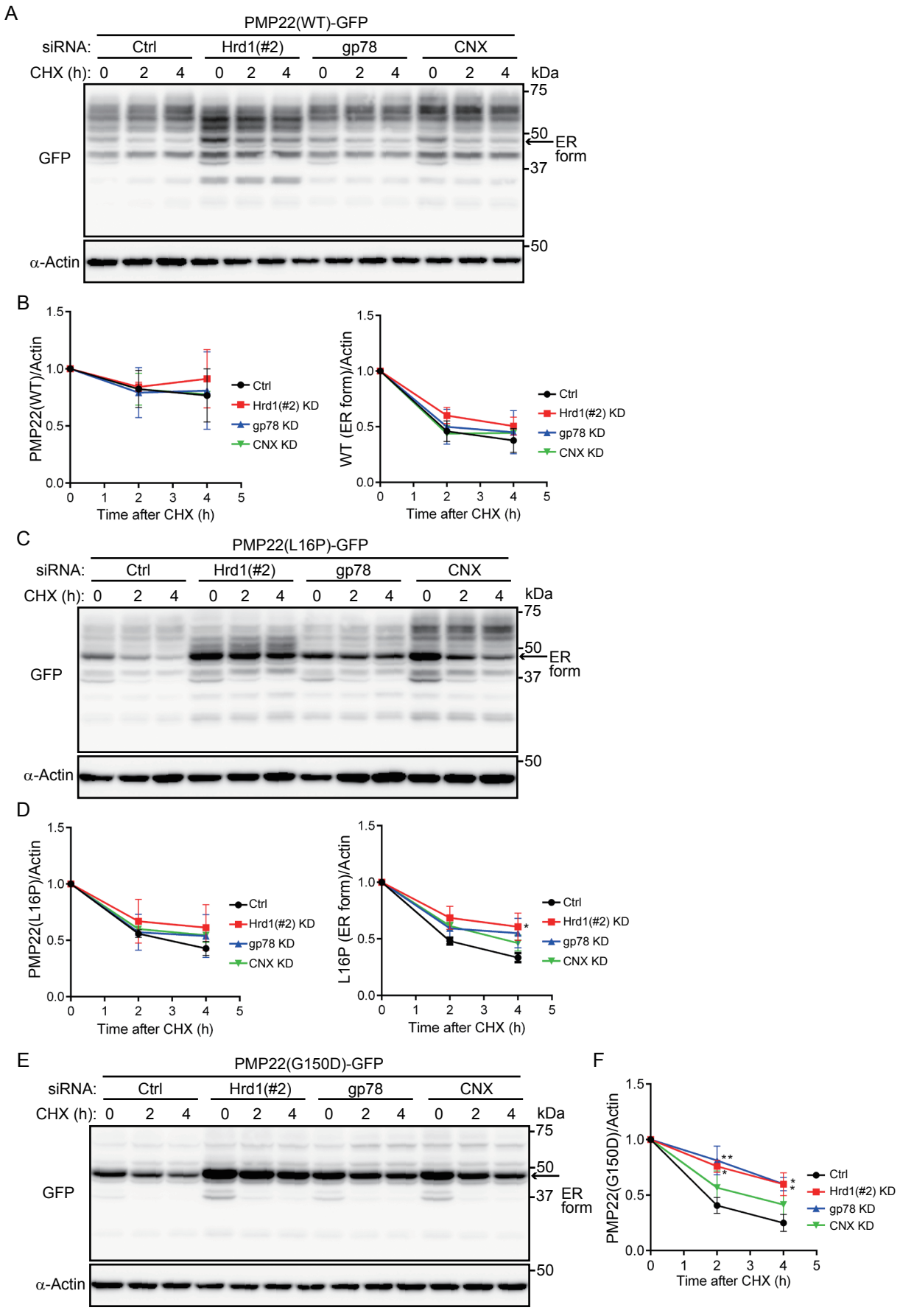


**Figure S3. Effect of *Hrd1*, *gp78*, and *calnexin* knockdown on PMP22 degradation.**

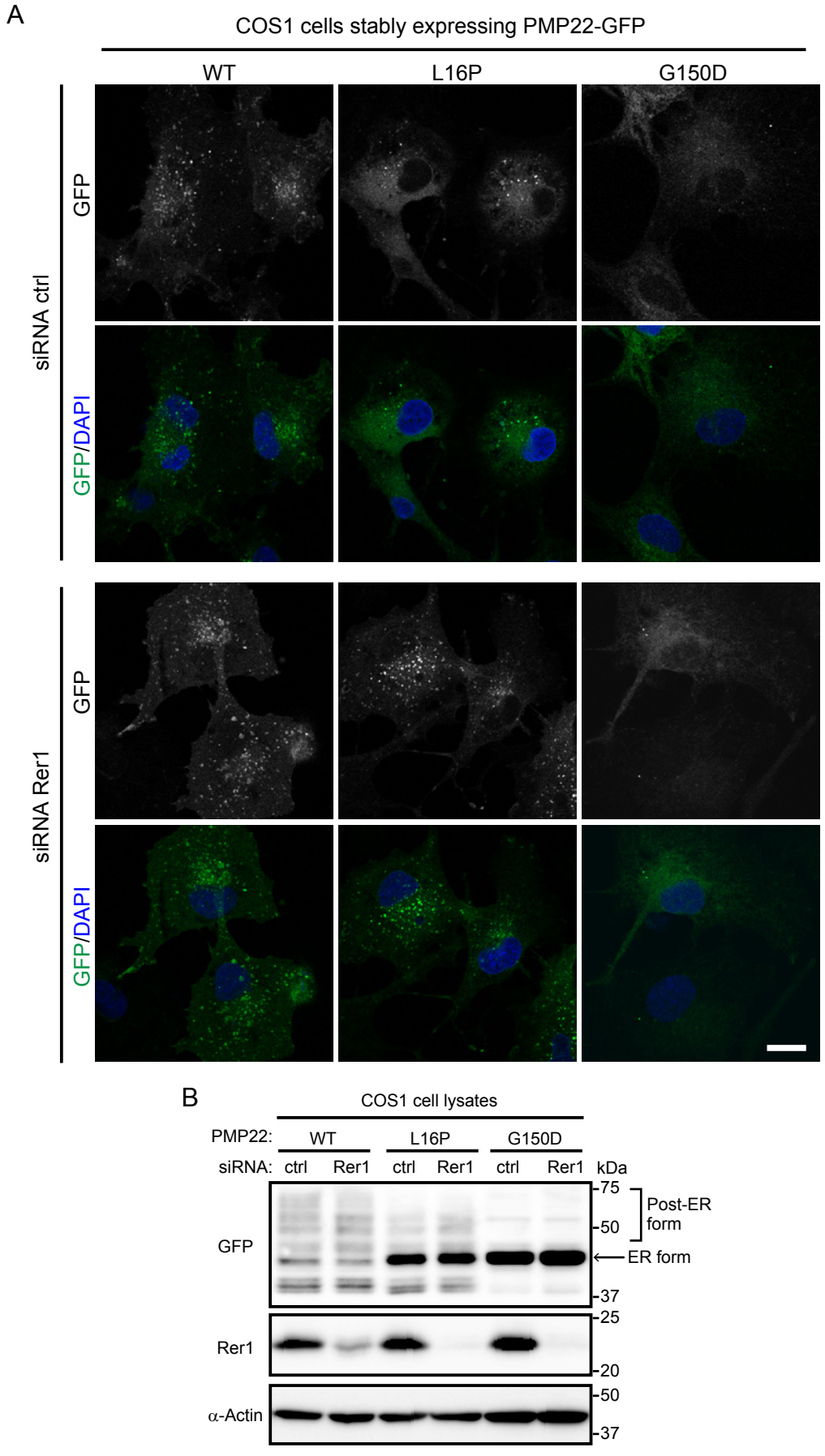


**Figure S4. Effect of *Rer1* knockdown on the ER retention of PMP22(L16P) in COS1 cells.**

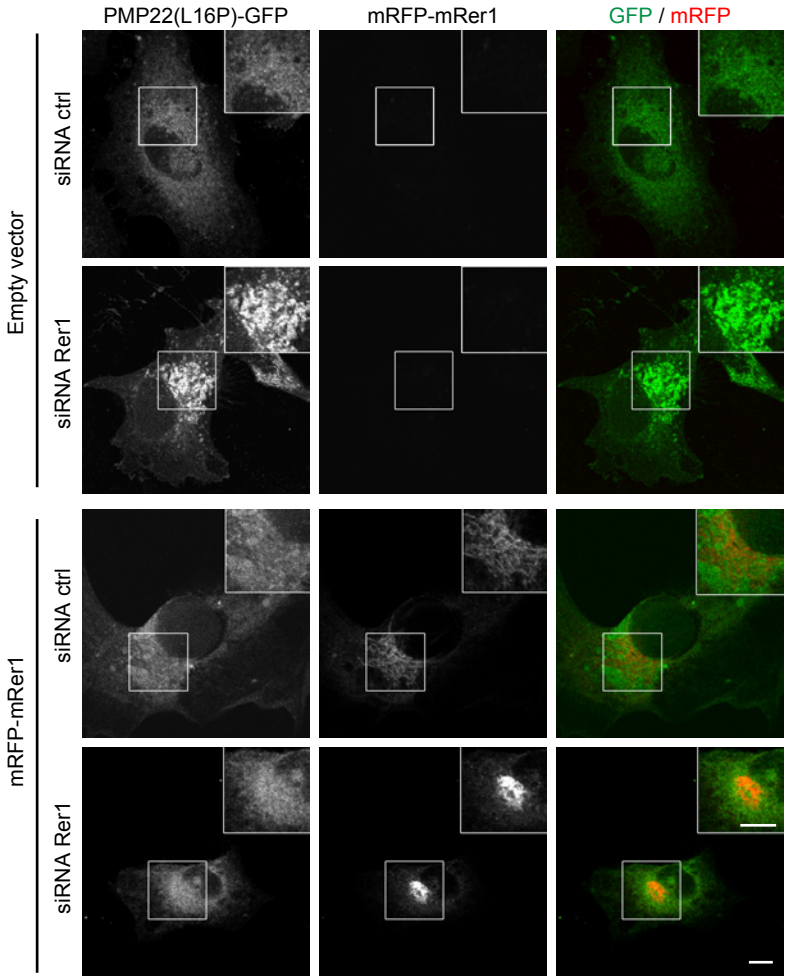


**Figure S5. Validation of the phenotype specificity induced by *Rer1* knockdown.**

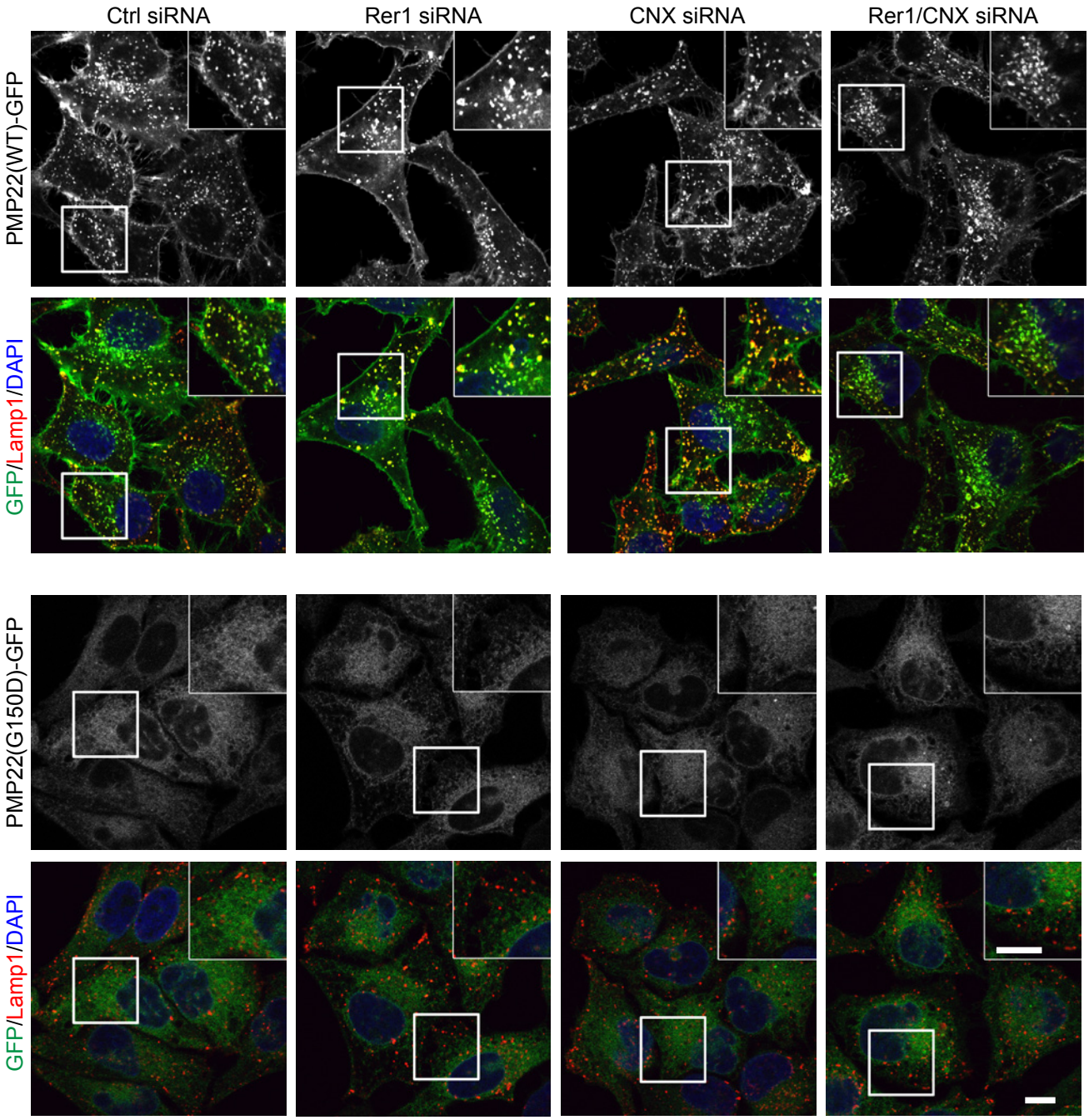


**Figure S6. Localization of PMP22(G150D)-GFP to the ER was superficially unaffected by simultaneous knockdown of *Rer1* and *calnexin*.**

Original gel images of Figure 1

Figure 1C

IB: GFP

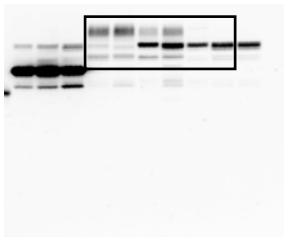

IB: GSK-3β

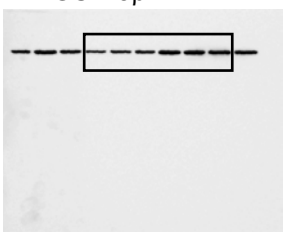

Figure 1D

IB: GFP

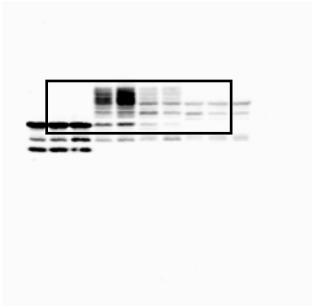

IB: GSK-3β

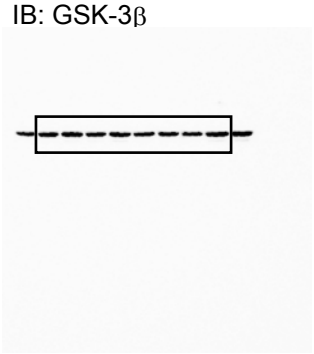

Original gel images of Figure 2

Figure 2A

IB: GFP

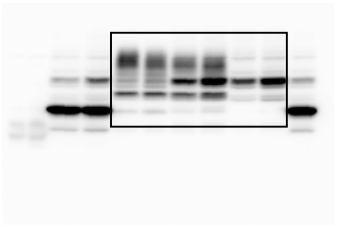

IB: α-Actin

IB: gp78

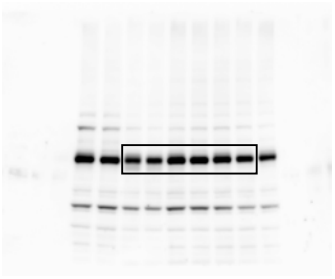

IB: Hrd1

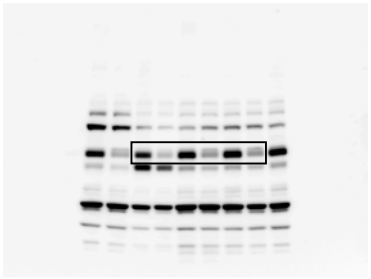

Figure 2B

IB: GFP

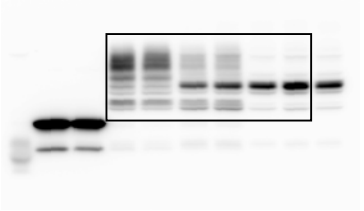

IB: α-Actin

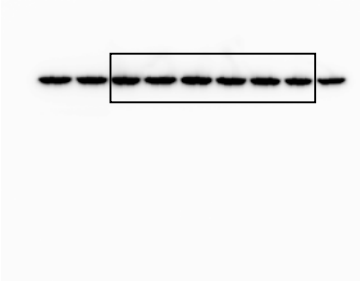

IB: gp78

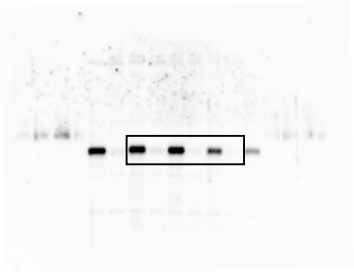

IB: Hrd1

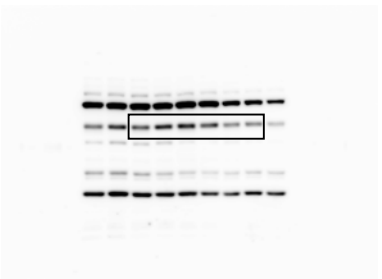

Figure 2E

IB: GFP

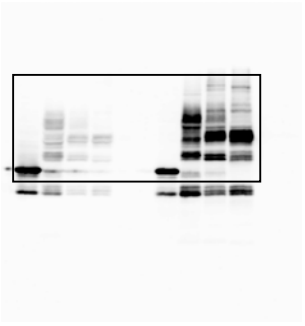

IB: Hrd1

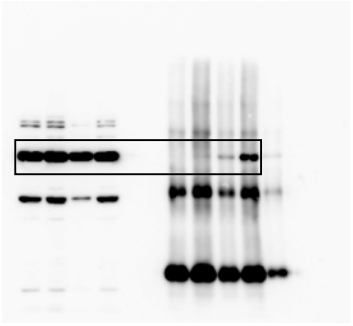

IB: gp78

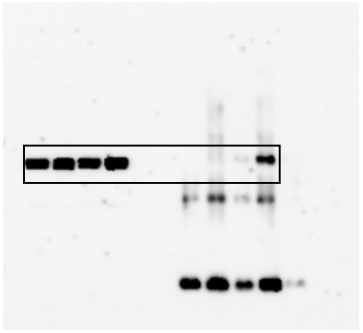

Figure 2F

IB: GFP

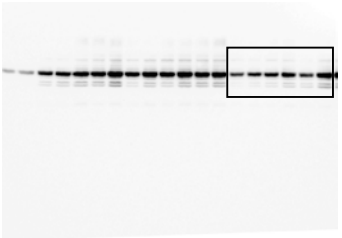

IB: α-Actin

IB: Hrd1

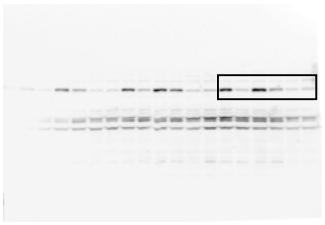

IB: gp78

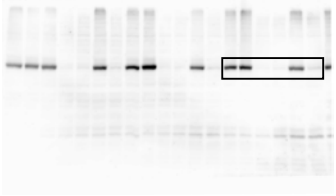

Original gel images of Figure 3

Figure 3A

IB: GFP

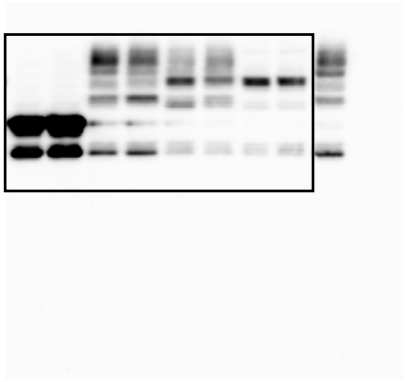

IB: Rer1

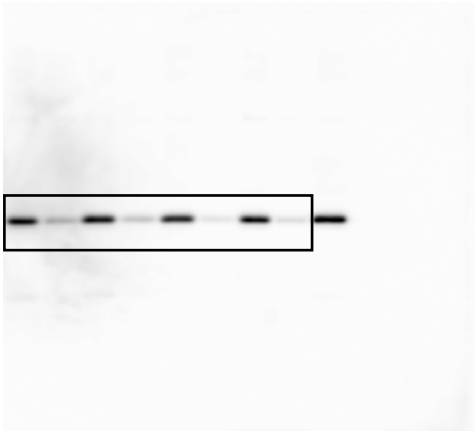

IB: α-Actin

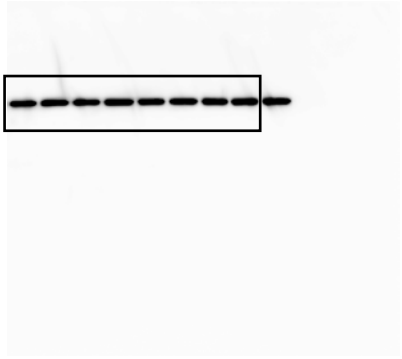

Figure 3B

IB: GFP

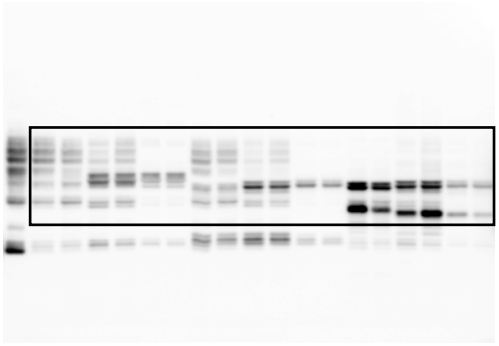

IB: Rer1

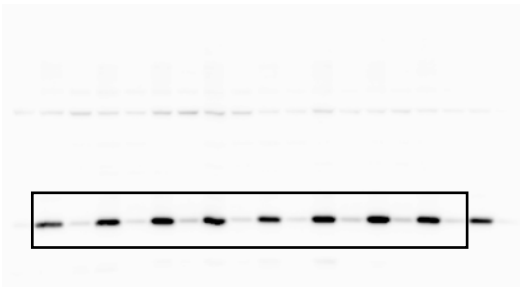

IB: α-Actin

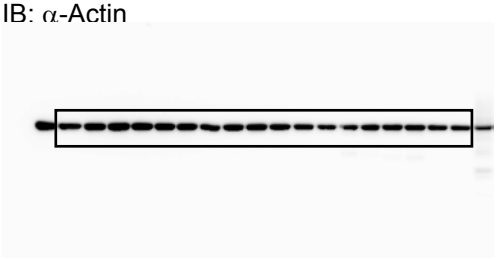

Original gel images of Figure 4

Figure 4A

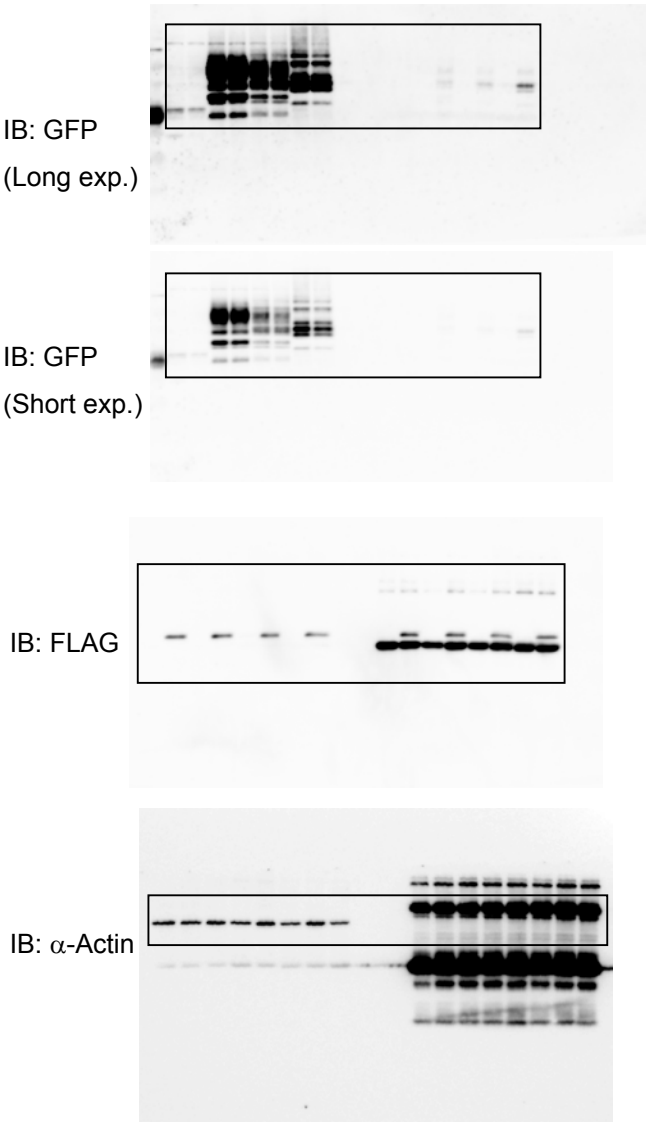


Figure 4B

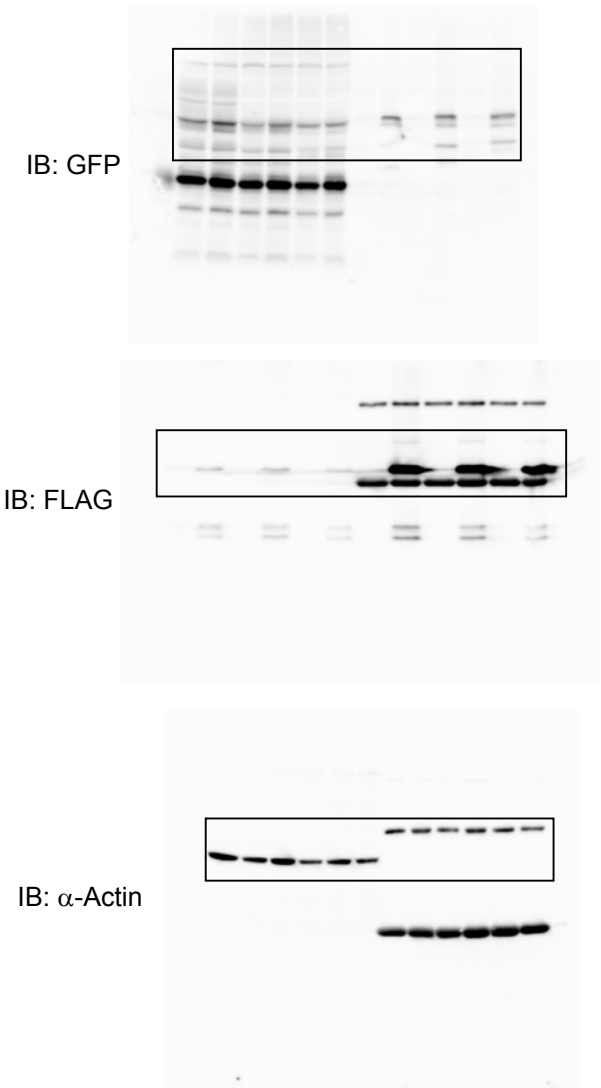

Original gel images of Figure 5

Figure 5A

IB: GFP

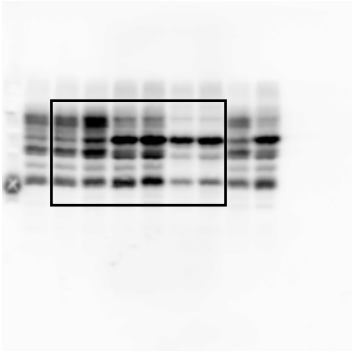

IB: CNX

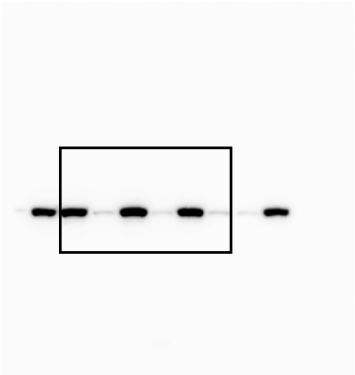

IB: α-Actin

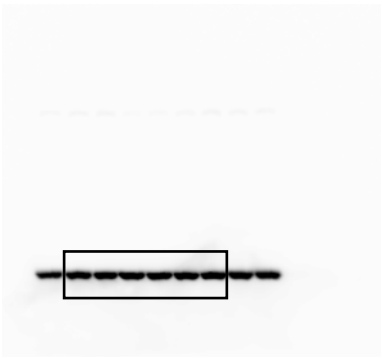

Original gel images of Figure 6

Figure 6A

IB: GFP

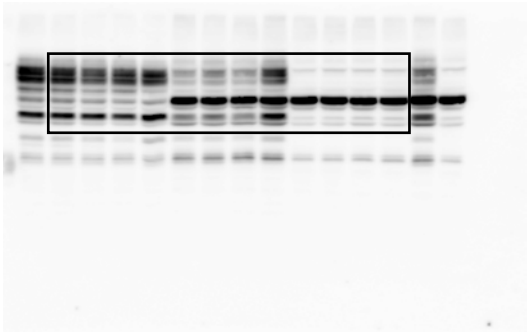

IB: α-Actin

IB: Rer1

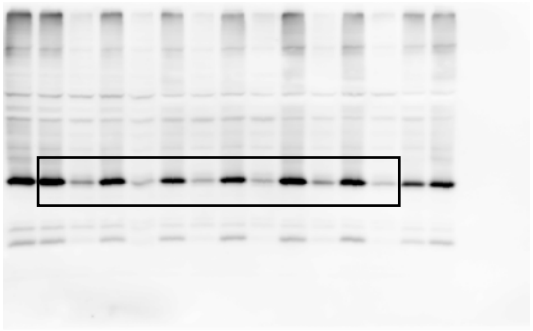

IB: CNX

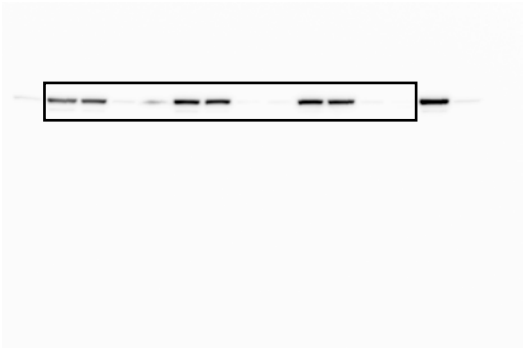

Figure 6C

IB: CNX

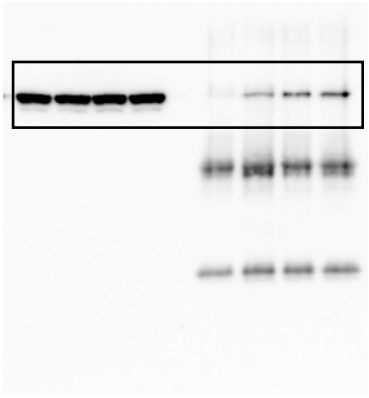

IB: GFP

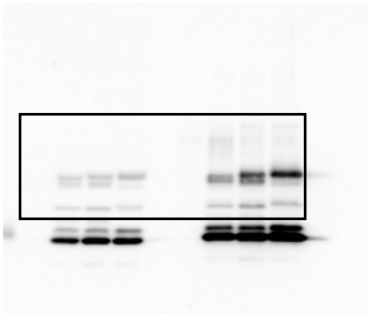

IB: Rer1